SSRG International Journal of Electrical and Electronics Engineering
ISSN: 2348-8379/ https://doi.org/10.14445/23488379/IJEEE-V12I8P121

Volume 12 Issue 8, 246-256, August 2025

Original Article

Performance Evaluation of Cascaded Converter-Based Hybrid Power Supply for PV-Assisted Light Electric Vehicle

R. Punyavathi[1], A. Pandian[2*], Vijaya Huchche[3], Nelluri China Kotaiah[4], Busireddy Hemanth Kumar[5*], Arvind R. Singh[6]

[1,3]*Department of Electrical and Electronics Engineering, Koneru Lakshmaiah Education Foundation, Guntur, India.*
[2]*Department of Electrical Engineering, Ramdeobaba University, Nagpur, India.*
[4]*Department of Electrical and Electronics Engineering, R.V.R&J.C College of Engineering, Guntur, India.*
[5]*Department of Electrical and Electronics Engineering, Mohan Babu University, Tirupati, A.P., India.*
[6]*Honorary Research Fellow, Applied Science Research Center and Applied Science Private University, Amman, Jordan.*

[*]*Corresponding Author : pands07@gmail.com*

Received: 16 June 2025 Revised: 17 July 2025 Accepted: 16 August 2025 Published: 30 August 2025

Abstract *- The lighter power electronic interface for PV, battery, and super capacitor-based power supply to PV-assisted light EV greatly enhances the drive system's efficiency. This paper presents a novel cascaded converter-based PV- Battery-Super capacitor power supply interface with reduced battery and supercapacitor power converters, which is controlled through model-referred Duty estimation-based PI control for maximum power absorption from PV source, accurate current reference generation for battery and super capacitor, faster current Control, and accurate DC bus regulation. The proposed converter interface and Control simulation were carried out in MATLAB/SIMULINK environment. Simulation results proved the robustness of Control with 2.7 percent regulation in DC bus voltage, 0.05 sec and 5 sec transient settlement times for supercapacitor and battery bus voltages.*

Keywords *- Solar electric vehicle, Model referred Control, PV-Battery interface, Super capacitor, EV drive.*

1. Introduction

Efficiency and size of the power train are the key factors for the productivity of a light motor solar electric vehicle. With the inclusion of a Photovoltaic (PV) source and battery power supply, the power electronic converter size determines the size of the power train. In this regard, the present study focuses on two aspects of power electronic interface for hybrid PV, battery and super capacitor power supply to Electric Vehicle (EV) motor drive. First, the study of topologies towards a lighter interface and second, efficient Control of the multiple source system. Sources such as Wind power, PV power, and power from a fuel cell [1] are reviewed for application to a light solar EV. Multi-input nonisolated converters are proposed for DC bus integration [2, 3] in which fuzzy logic control determines the coordinated power share. Battery storage, super capacitor assistance [4], and combined with Control for average and ripple currents, has been developed. The features of bi-directional power flow are provided to the interfacing converters to facilitate regeneration during braking operation [5]. Interfacing the DC bus with three-level converters is developed [6] with reduced component size. Usage of the same interface for battery charging is developed [7], which also facilitates charging operation with high efficiency. Another vertical in topologies is identified with the power from multiple sources being integrated in a single stage conversion [8]. This method has an additional advantage: it does not need a Maximum Power Point Tracking (MPPT) DC-DC converter. Further, there are processes which aimed at optimal size of power sources [9], power conversion in both the directions [10], and inclusion of multiple functions for one converter [11, 12] analyzing thermal withstand capabilities [13, 14] and inclusion of other functions for the main power converters [15, 16]. All these topologies have the merits of multiple source interfaces, but at the cost of a complex interface.

On the other hand, numerous control techniques are reported. Heuristic approaches like machine learning [17], load prediction-based schedule of energy supply [18], power supply schedule upon C-rate and PV power conditions [19] aimed at coordinated power sharing in hybrid power supply to meet gradual and sudden changes in load demand. Other approaches are also proposed, such as model predictive current reference generation [20], estimation of power

demand based on drive cycle and subsequent generation of sharing function for sources [21], and anticipatory demand control [22] for control coordination in the hybrid power supply system. Machine learning is the more recent inclusion in control coordination machine learning [23], supervised learning for determining power converter parameters [24], and combined energy hub [25, 26] are reported in the latest control algorithms.

Therefore, it is found that the front-end hybrid power supply for DC bus-based power electronic applications needs better regulation, quick transient settlement, and reduced overall interface size to make it adoptable and efficient for drive or other DC bus-based power conversion systems. The challenges in this process include designing shared converter resources for power conversion and implementing feed-forward Control. With these findings, the present work proposes a cascaded converter topology and a model referred to as duty estimation in PI-regulated closed-loop control of a hybrid power supply system for an efficient and cost-effective solution for PV-battery-super capacitor interface for light solar EV.

The novel contributions of the work include:

- Development of a two-stage cascaded power conversion topology for integrating battery and supercapacitor into the DC bus.
- This reduced the size of the inductor for integrating a battery into a hybrid power supply system.
- This also reduced stress on the power switches of the battery interface compared to conventional interfaces.
- Development of a novel control algorithm that determines the instantaneous duty cycle through converter dynamic equations for PI-based closed-loop DC bus regulation.
- Better regulation of the DC bus and super capacitor bus with proposed Control.

The rest of the paper is organized as follows. Section 2 presents the topology and mathematical model of the proposed two-stage cascaded converter-based power supply. Section 3 presents the control structure for the proposed converter. Section 4 presents simulation results and performance validation of the system. Section 5 presents the conclusion of the paper.

2. Model of Cascaded Converter Hybrid Power Supply System

The primary objective is to develop a novel topology with reduced size of power switches and filter components for a stage conversion of Battery power for interfacing PV and Battery sources to the electric vehicle power train. The conventional integration includes the injection of power from a PV source, battery and super capacitor into the DC bus of the drive as parallel components, as shown in Figure 1. Bi-directional power control converters are employed for integrating the battery source power and supercapacitor into the DC bus. Series and parallel switches in these converters facilitate respective buck or boost operation. The modified topology, which integrates a super capacitor in one stage and battery power in two stages into the DC bus, is shown in Figure 2. With the converter for PV integration remaining the same as the conventional process, the battery power integration is modified as a two-stage process. In the first stage, the battery supplies power to the super capacitor bus. In the second stage, the super capacitor bus supplies battery power and power from the super capacitor to the DC bus. In this process, the sizing of the converters in each of the cascaded stages is reduced significantly for a performance similar to that of conventional integration. This size reduction is due to the change in Bus voltage levels between which the converters are placed compared to conventional integration.

2.1. Duty Generator for Conventional Converter

The equivalent voltage across the inductor condition of the PV converter when the switch S_{PV} is ON is given as V_{PV}. During this condition, The dynamics of the PV converter are depicted in Equations (1)

$$\frac{di_{PV}}{dt} = \frac{V_{PV}}{L_{PV}} \tag{1}$$

The output current of the PV array as a function of terminal voltage is given as

$$i_{PV} = i_{SC}(e^{AV_{PV}} - 1) \tag{2}$$

Where A is the material constant of the PV panel.

The condition for extracting maximum power from P-V and I-V curves is obtained as

$$\frac{dP_{PV}}{di_{PV}} = 0 \text{ and } \frac{dV_{PV}}{di_{PV}} = 0 \tag{3}$$

Considering P_{PV} V_{PV}. i_{PV},

$$\frac{dP_{PV}}{di_{PV}} = \frac{d}{dt}(V_{PV} i_{PV}) = V_{PV} + i_{PV}\frac{d}{di_{PV}}V_{PV} \tag{4}$$

Therefore, at maximum power condition,

$$\frac{dV_{PV}}{di_{PV}} + \frac{V_{PV}}{i_{PV}} = 0 \tag{5}$$

In the real-time sampling, Equations (1) and (5) were considered as

$$\frac{i_{PV}(k+1) - i_{PV}(k)}{d_{PV} T_S} = \frac{V_{PV}(k)}{L_{PV}} \tag{6}$$

$$\frac{V_{PV}(k+1) - V_{PV}(k)}{i_{PV}(k+1) - i_{PV}(k))} + \frac{V_{PV}(k)}{i_{PV}(k)} = 0 \tag{7}$$

Thus, the Duty for the next sampling instant is obtained from equations (6) and (7).

The dynamics of the Battery converter are depicted in Equations (8) and (9) as follows:

$$L_{Bat}\frac{di_{Bat}(t)}{dt} = V_{Bat}(t) - d_2(t)V_{Bus}(t) \quad (8)$$

In real-time sampling, these are considered as,

$$L_{Bat}\frac{i_{Bat}(k+1)-i_{Bat}(k)}{t_s} = V_{Bat}(k) - d_2(k+1)V_{Bus}(k) \quad (9)$$

Given the reference value of current i_{Bat}^*, the duty ratio needed for the next sample is given as

$$d_2(k+1) = \frac{V_{Bat}(k)}{V_{Bus}(k)} - \frac{L_{Bat}i_{Bat}^*}{t_sV_{Bus}(k)} + \frac{L_{Bat}i_{Bat}(k)}{t_sV_{Bus}(k)} \quad (10)$$

The dynamics of the super capacitor converter are depicted in Equations (11) and (12) as follows:

$$L_{sc}\frac{di_{sc}(t)}{dt} = V_{sc}(t) - d_1(t)V_{Bus}(t) \quad (11)$$

Discretizing the differential equation,

$$L_{sc}\frac{i_{sc}(k+1)-i_{sc}(k)}{t_s} = V_{sc}(k) - d_1(k+1)V_{Bus}(k) \quad (12)$$

Given the reference value of current i_{sc}^*, the duty ratio needed for the next sample is obtained as:

$$d_1(k+1) = \frac{V_{sc}(k)}{V_{Bus}(k)} - \frac{L_{sc}i_{sc}^*}{t_sV_{Bus}(k)} + \frac{L_{sc}i_{sc}(k)}{t_sV_{Bus}(k)} \quad (13)$$

2.2. Duty Generator for Proposed Interface

Owing to the connections of the PV converter and super capacitor converter connected to DC bus remained same in proposed two stage cascaded converter for battery interface to DC bus the equations pertaining to duty cycle generation for dc-dc converter of PV source and super converter between super capacitor and DC bus remain same as Equations (9) and (10) respectively. The dynamics of stage 1 conversion are depicted in Equations (14) and (15) as follows:

$$L_{Bat}\frac{di_{Bat}(t)}{dt} = V_{Bat}(t) - d_2(t)V_{Bus}(t) \quad (14)$$

In real-time sampling, it is considered as,

$$L_{Bat}\frac{i_{Bat}(k+1)-i_{Bat}(k)}{t_s} = V_{Bat}(k) - d_2(t)V_{Bus}(k) \quad (15)$$

The duty ratio needed for the next sampling instant is obtained as

$$d_2(k+1) = \frac{V_{Bat}(k)}{V_{sc}(k)} - \frac{L_{Bat}i_{Bat}^*}{t_sV_{sc}(k)} + \frac{L_{Bat}i_{Bat}(k)}{t_sV_{sc}(k)} \quad (16)$$

3. Model-Derived Duty-Based Control

A novel control structure that utilizes proportional Plus Integral (PI) control for generating a current reference is developed. Then, the duty ratio for the successive sampling interval is determined from the converter model. The objectives of the control algorithm are: absorption of maximum power from the PV source pertaining to available irradiation, DC bus voltage, and coordinated power sharing. The Model-Based Duty (MBD) control is depicted in Figure 3. The PV interface converter is independently controlled with respect to the battery and super capacitor converters. This converter always feeds the DC bus with maximum available power at any given instant. The other two sources, viz. battery and super capacitor, should share the rest of the power demand per load at any given instant. The proposed current regulation scheme is explained as follows:

The control algorithm has two stages: generating reference currents for the battery and supercapacitor, and obtaining respective gating control signals. The DC bus regulation error given to the PI controller provides a reference current to be generated. The average value of the reference current is given as a reference to the battery converter inductor. The ripple extracted from the reference current is given as a reference to the supercapacitor converter. Gating control pulses for SPV are obtained from the PV converter model as described in Equations (6) and (7). The voltage and current obtained from the MPP algorithm decide the current reference, and Equation (7) determines the respective duty ratio for the next sampling interval. Similarly, dynamics provided in (10) and (13) generate the next sample duty ratio for the battery converter and super capacitor converter, respectively. These duty ratio signals are modulated with constant frequency carriers to generate switching pulses for S_1 and S_2. The complementary waveforms are fed to S_3 and S_4, respectively. Modifications are made to control proposed for conventional topology to apply for proposed cascaded converter topology are shown in Figure 4. Firstly, the d2nom now varies as compared to conventional converter, as it is placed between battery and super capacitor instead of between battery and DC bus. Therefore, it is modified by the equivalent factor as d2nom * (Vsc/VBus). Also, Equation (16) serves as a reference to generate the duty cycle for the super capacitor-DC bus converter and Equations (10) and for the PV converter are similar to Equations (6) and (7).

4. Simulation Results and Performance Evaluation

The cascaded converter with MDD control scheme and the control scheme's application to conventional topology were simulated in MATLAB/SIMULINK. A resistive load controlled by an external signal source was considered to provide a time-varying load similar to electric vehicle drive cycles, including acceleration, constant velocity and vehicle deceleration. The system simulation parameters are provided in Table 1, which includes parameters of sources and filter

elements. The non-ideal nature, such as series parasitic resistance for filter components, is considered to be 0.5 percent of its nominal value. Power switches are considered with a snubber and parasitic ON state resistance.

Table 1. Simulation parameters

Parameter	Simulation
Load	500 W – 1 kW
PV Specifications	2 x (36 V, 9.8 A, 330 W_p)
Battery Specifications	I_{max}= 20 A, $V_{nominal}$= 12 V, Capacity =200 AH
Super Capacitor Capacitance	58 F
Super Capacitor Voltage	18 V
DC Bus Specifications	48 V
L_{Bat}	0.8 mH
L_{PV}	1 mH
L_{sc}	1 mH
C_{DC}	440 µF
PI Coefficients	0.0325, 0.224

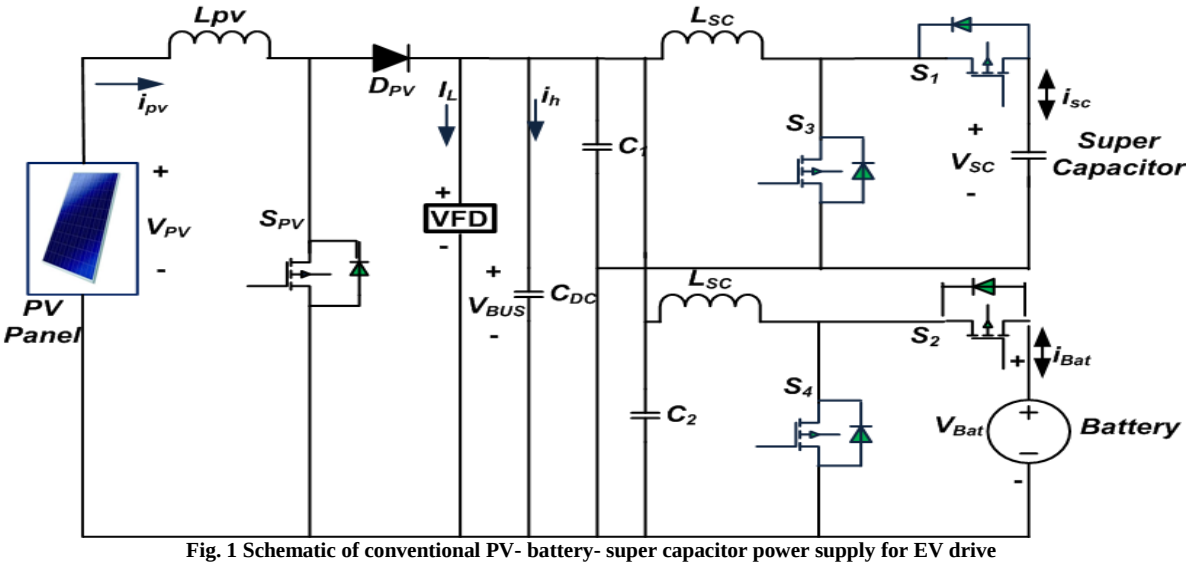

Fig. 1 Schematic of conventional PV- battery- super capacitor power supply for EV drive

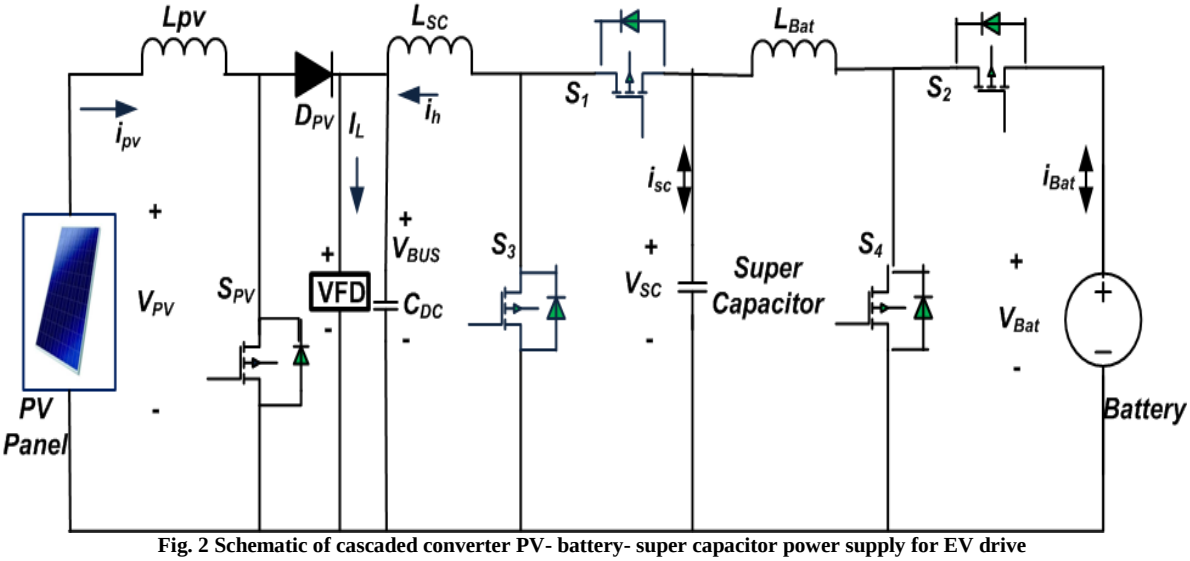

Fig. 2 Schematic of cascaded converter PV- battery- super capacitor power supply for EV drive

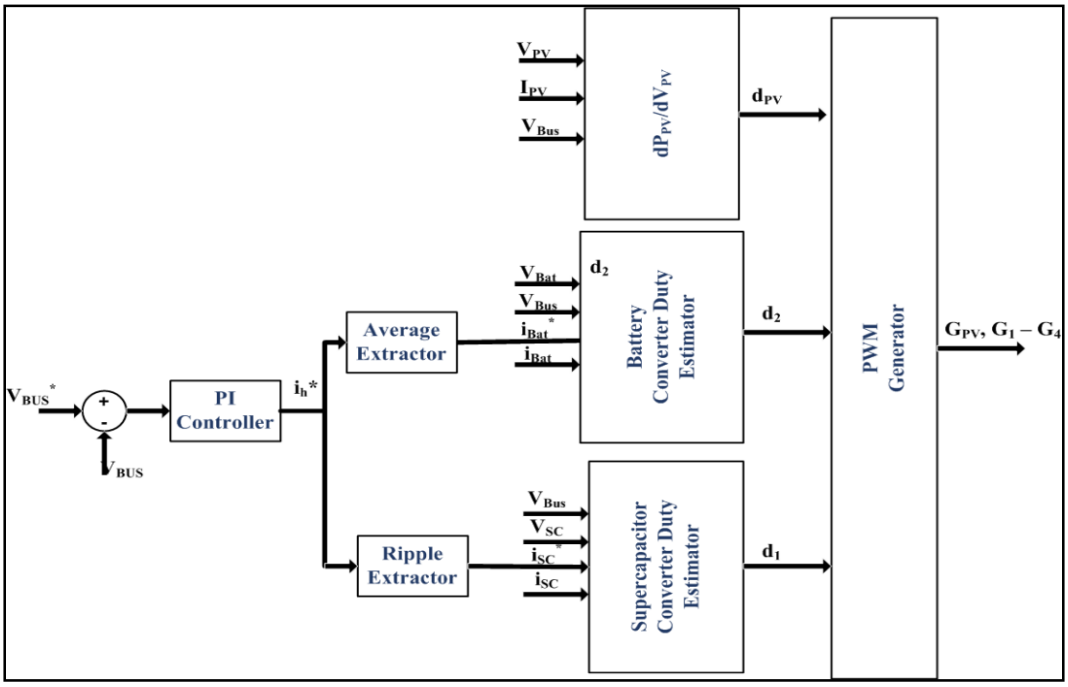

Fig. 3 Model-derived duty-based current control for conventional topology

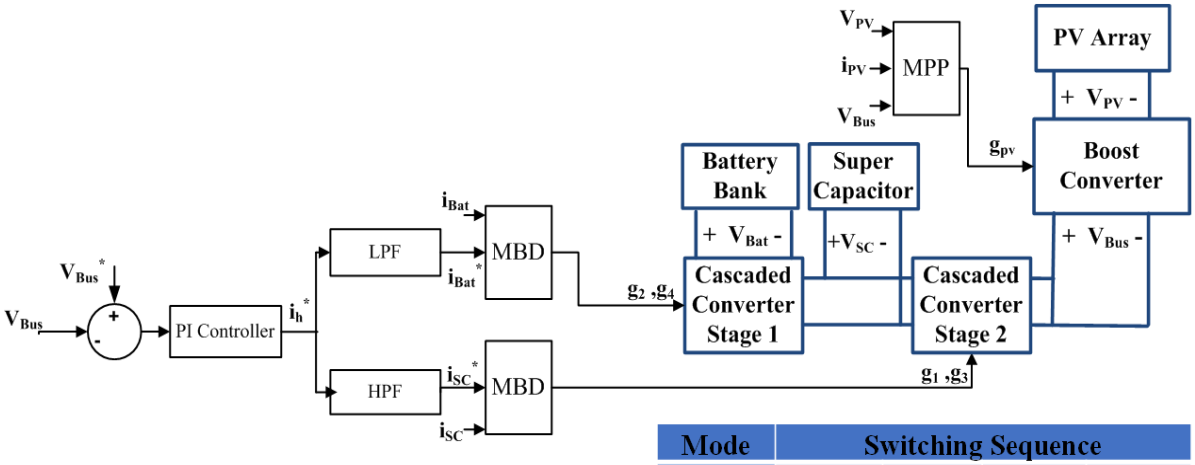

Mode	Switching Sequence			
	S2	S4	S1	S3
S1US2U	PWM	1	PWM	1
S1DS2U	0	PWM	PWM	1
S1US2D	PWM	1	0	PWM
S1DS2D	0	PWM	0	PWM

Fig. 4 Model-derived duty current control for cascaded converter topology

4.1. Current and Power Sharing Performance

As stated in previous section a random signal-controlled resistance created a load current demand as shown in Figure 5. The current supplied by PV source is according to MPP algorithm at varying irradiance as seen from Figure 5. The rest of current demand by the load is supplied by combination of battery and super capacitor as shown in Figure 5. Owing to the slower response of battery current because of its chemical properties it can be seen from Figure 5 that at instants where there is sudden increase in load current such as at time interval near to 50 sec and sudden decrease in load current demand such as at time interval near to 230 sec, respective c-rate of the battery limits current of the battery. At such instances, the reaction of the super capacitor could be absorbed in terms of a sudden supply of current or sudden absorption of current to meet the load demand. During constant load current which is

met by battery and PV current, super capacitor only floats without any power supply or absorption which can be observed from Figure 5. Also, for gradual increase or decrease of load current, battery current is adjusted quickly to meet the load demand as seen from Figure 5 at intervals 120 – 125 sec and 180 – 190 sec respectively. A similar response is observed with conventional topology as well. Voltages at the DC bus, super capacitor bus and battery bank are shown in Figure 6, which are regulated to the designed magnitude with accurate tracking observed from Figure 6. The regulation and voltage stress are discussed in detail in the next subsection. A highly accurate regulation is observed for various load values, accounting for a magnitude close to five percent. With voltages regulated very accurately to nominal values, it is evident from Figure 7 that the power share among the sources follows a pattern similar to the current share. It is also evident from Figure 7 that the irradiance-dependent PV power is supplied to the DC bus. The rest of the power demand is shared between the battery and the super capacitor. Similar to the response of current, the sudden variations in load power are instantaneously tackled by the super capacitor while the battery adjusts to meet the corresponding load power demand.

4.2. DC Bus Regulation and Super Capacitor Voltage Stress Performance

From the variations of load power demand, a worst-case sudden decrease in load is considered at 150 sec. Owing to this sudden change, the DC bus voltage pertaining to conventional converter topology is shown in Figure 8. The DC bus voltage is raised to 49.9 V and is regulated to the nominal 48 V at 155 sec. Therefore, the worst-case voltage regulation in this case is obtained as 3.125 percent, and the transient time for settling back is 5 sec. The similar load change for the cascaded converter topology resulted in a DC bus voltage change, as shown in the Figure. 9. The DC bus voltage is raised to 48.9 V and is regulated to a nominal 48 V at 155 sec. Therefore, the worst-case voltage regulation in this case is obtained as 2.7 percent, and the transient time for settling back is 5 sec. Thus, the cascaded converter topology resulted in better voltage regulation for the worst-case variation in the nominal range load. Similarly, the voltage stress on the supercapacitor is also studied. In this case, the worst-case demand is observed at 40 seconds when the load suddenly increases. An instantaneous drop in voltage to 17.69 V followed by a rise to 18.32 V is observed for the super capacitor voltage with a conventional converter topology as shown in Figure 10. The percentage voltage stress for this worst-case variation is obtained to be 2.2 percent. For a similar situation, with a cascaded converter topology, an instantaneous drop in voltage to 17.95 V is observed, as shown in Figure 11. In this case, the percentage voltage stress is only 1.6 percent. Thus, along with better DC bus regulation, the super capacitor's voltage stress performance is also improved with cascaded converter topology by applying the proposed Control. A comparison is made to evaluate the DC bus regulation performance with existing topologies and proposed topologies with proposed Control. The existing topologies and predictive Control [2], heuristic Control [4], and hybrid Control [6] shown regulation of the order 12.5 percent to 4.25 percent whereas proposed Control to conventional topology is 3.125 percent and proposed cascaded converter with proposed model referred Duty estimated PI current control proved only 2.7 percent regulation as observed from Table 2. Also, the voltage stress on the super capacitor is decreased by 0.6 Percent with the cascaded converter topology, as seen from Table 3.

4.3. Battery Interface Sizing Comparison

The performance of filters and switches is evaluated in this section. The size of the filter inductor for the conventional battery interface from Equation (8) is obtained as:

$$L_{Bat} = \frac{V_{Bus}(V_{Bus}-V_{Bat})}{\Delta i_{LBat} f_s V_{Bat}} \tag{17}$$

Similarly, the size of the filter inductor for the proposed cascaded converter topology from Equation (14) is obtained as

$$L_{Bat} = \frac{V_{sc}(V_{sc}-V_{bat})}{\Delta i_{LBat} f_s V_{Bat}} \tag{18}$$

Substituting the considered nominal values for V_{Bus}, V_{Bat}, and V_{sc}

$$L_{Bat} = \frac{144}{\Delta i_{LBat} f_s} \tag{19}$$

Similarly, for the proposed cascaded converter topology,

$$L_{Bat} = \frac{9}{\Delta i_{LBat} f_s} \tag{20}$$

Therefore, the reduction in filter inductor size is determined in terms of percentage change, which is obtained as 93.75 percent. The above sizing calculations are evident from the Figures 12 and 13 that for 0.8 mH of battery interface inductor the steady state ripple in battery interface inductor current with conventional topology is observed to be 0.24 A as seen from Figure 12 and that with cascaded converter topology is observed to be only 0.14 A as seen from Figure 13 which proves the change in Δi_{LBat} For the same inductor size. A comparison is made to evaluate the sizing of the battery interface converter. The inductor at the battery interface, as calculated from (19) and (20) and verified from Figures 12 and 13, shows that a great reduction in inductor size is obtained with the cascaded converter. Also, the series switch S2 is evaluated for voltage stress at the OFF condition. Considering the voltage stress with conventional topology as 1 per unit, the voltage stress with cascaded converter topology is obtained to be only 0.16 per unit, as shown in Table 4. Therefore, a reduction in the sizing of battery interface components with equivalent performance is achieved with the cascaded converter with MBD control.

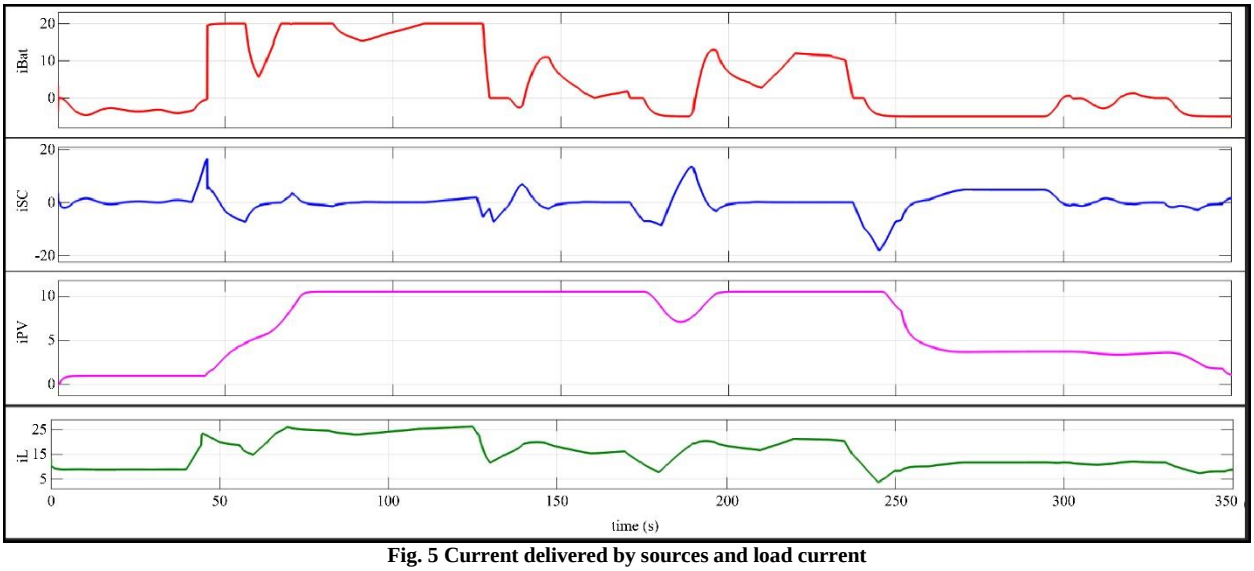

Fig. 5 Current delivered by sources and load current

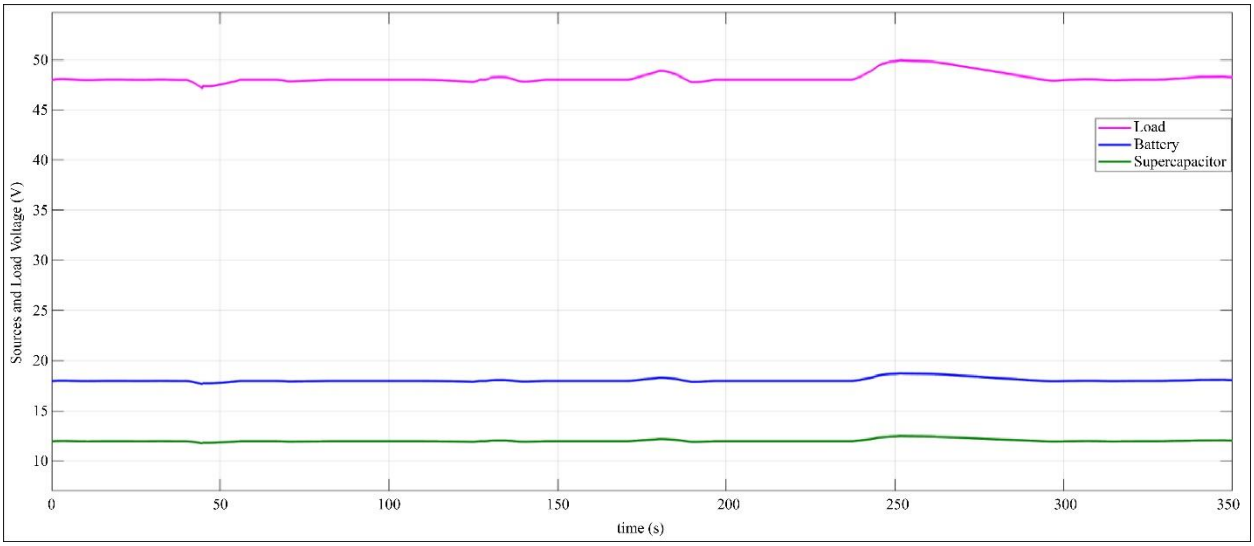

Fig. 6 Voltage of DC bus, super capacitor and battery bank

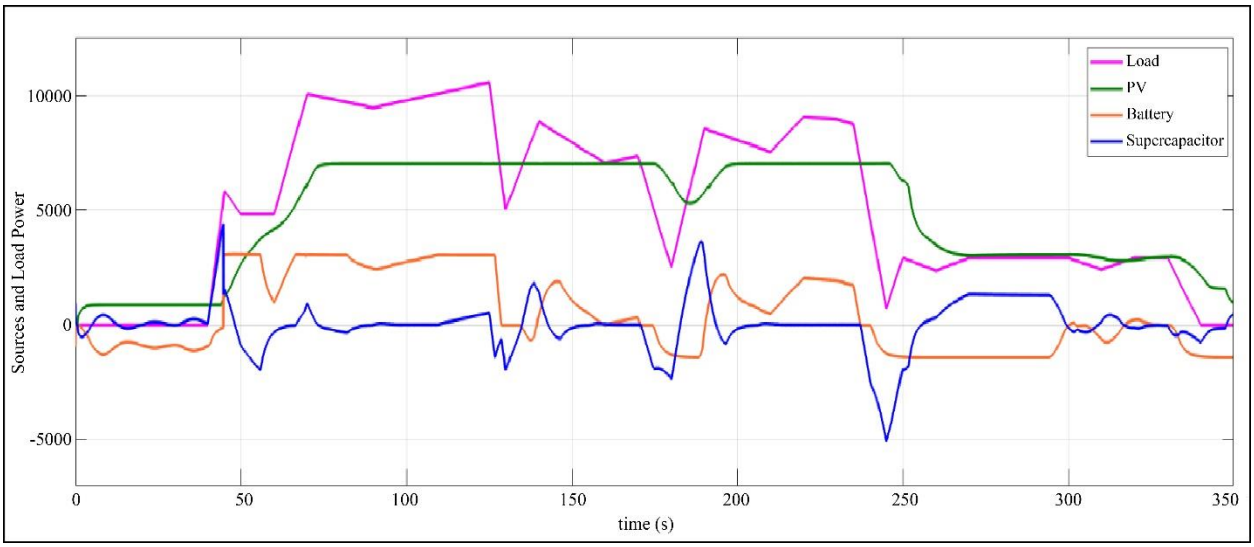

Fig. 7 Power associated with PV, battery, super capacitor and load bus

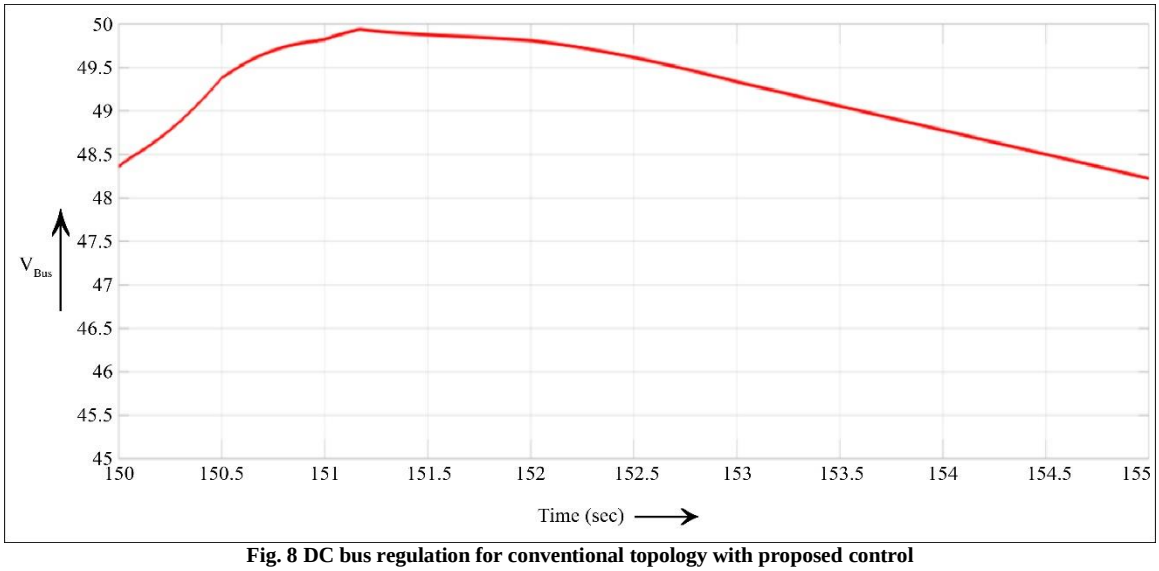

Fig. 8 DC bus regulation for conventional topology with proposed control

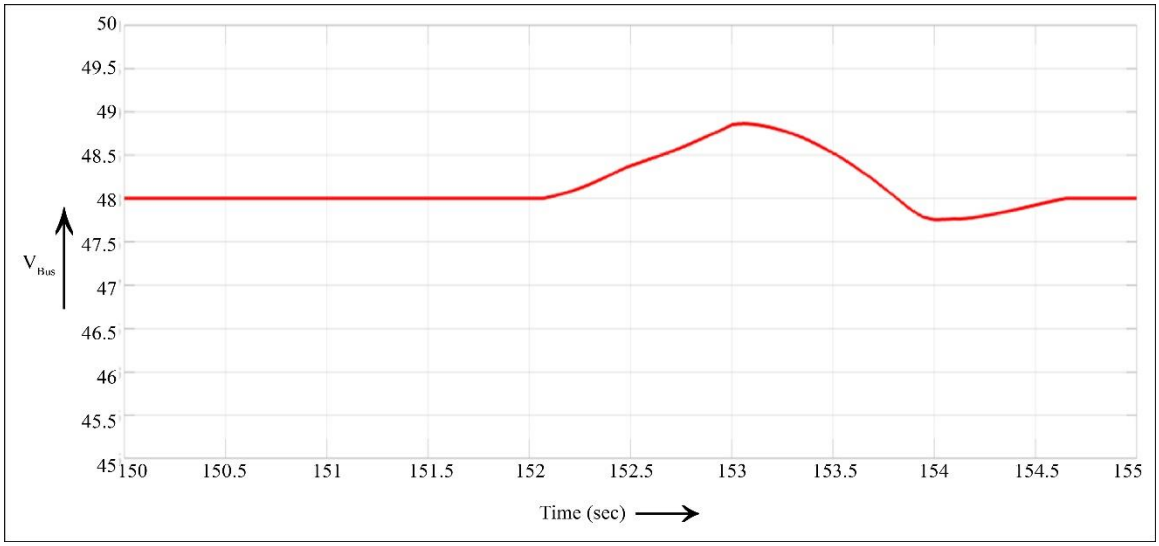

Fig. 9 DC bus regulation for cascaded converter topology with proposed control

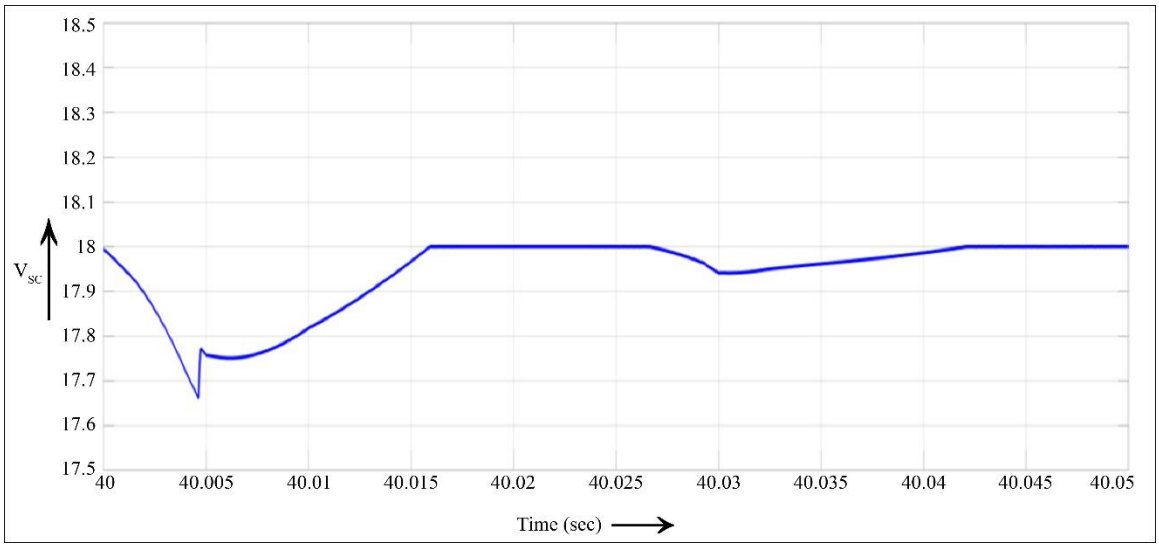

Fig. 10 Super capacitor voltage stress for conventional topology with proposed control

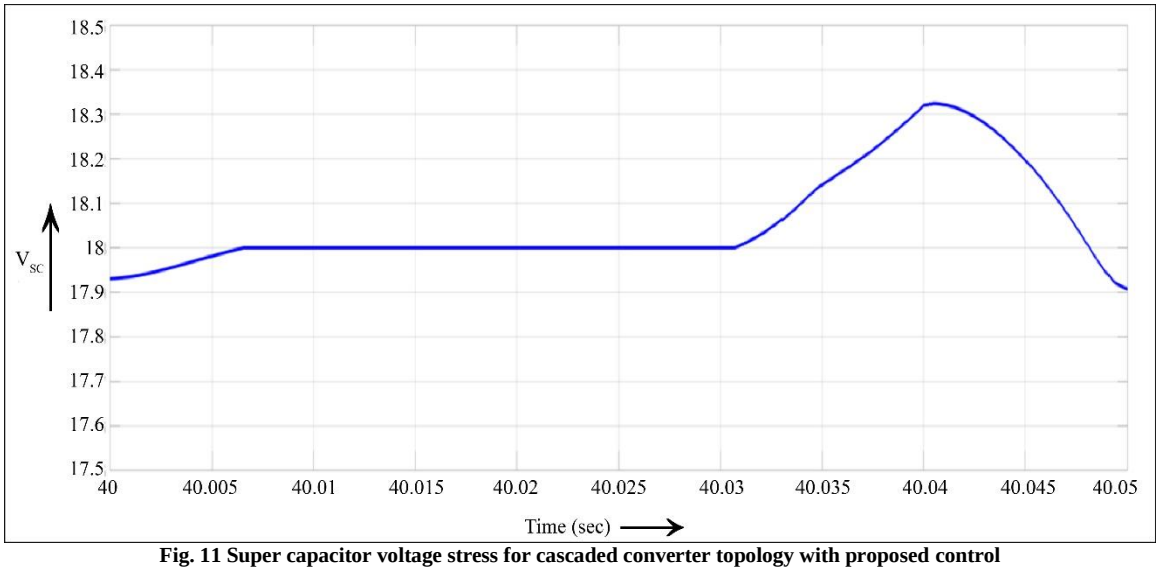

Fig. 11 Super capacitor voltage stress for cascaded converter topology with proposed control

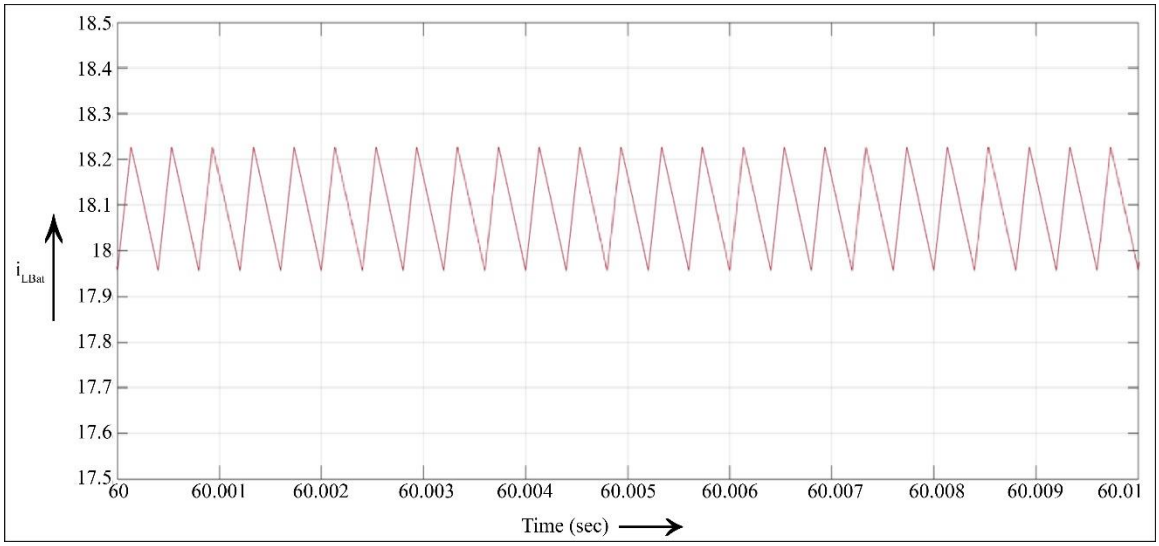

Fig. 12 Battery converter inductor current ripple with conventional topology

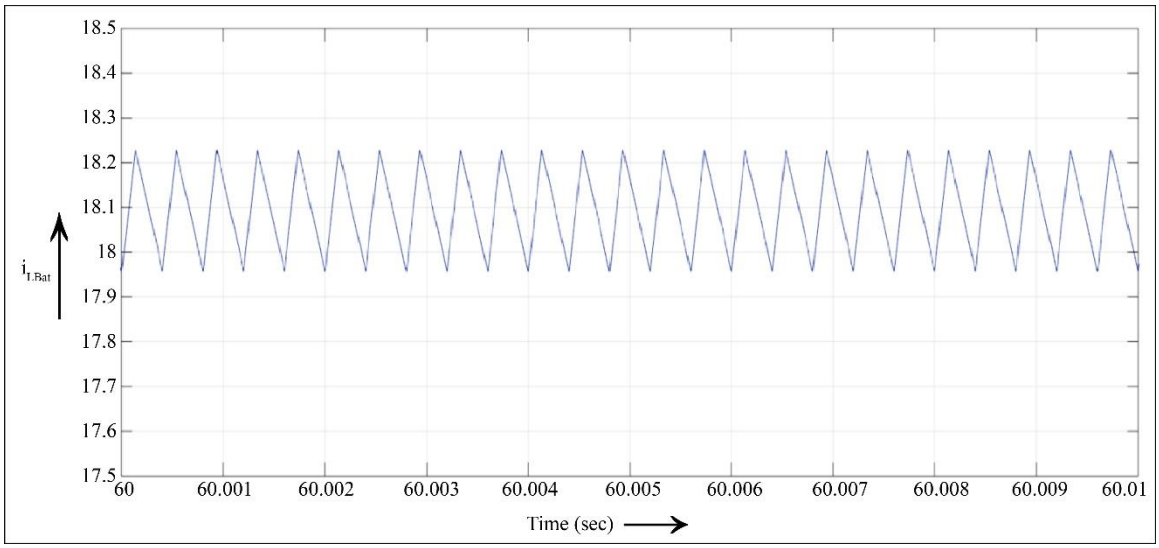

Fig. 13 Battery converter inductor current ripple with cascaded converter topology

Table 2. Comparison of DC bus regulation

	[2]	[4]	[6]	Conventional Converters with MDD control	Proposed Control for Cascaded Converter with MDD Control
Nominal Power (W)	480	40	80	900	900
Nominal DC Bus Voltage (V)	48	48	48	48	48
% DC Bus Voltage Regulation	12	5	4	3.225	2.75

Table 3. Comparison of super capacitor voltage stress

	Conventional Converters with MDD Control	Cascaded Converters with MDD Control
Capacitance (F)	58	58
Voltage (V)	18	18
Voltage Stress (%)	2.2	1.6

Table 4. Battery interface converter parameters comparison

	Conventional Converter	Proposed Cascaded Converter
Sizing of second stage inductor (mH)	0.8	0.56
Sizing of Switching voltage stress (pu)	1	0.16

5. Conclusion

The outlined seven-level MLI presents an efficient and novel cascaded converter-based topology for the interface of a PV- Battery-Super capacitor hybrid power supply for electric vehicle drive. A mathematical model for estimating the duty cycle of power switches in the topology is presented. A novel PI current control scheme with model-referred duty estimation is proposed and implemented.

The scheme is also implemented for the conventional interface. The MATLAB/SIMULINK platform is utilized for a simulation study. A good power sharing performance with a 0.05 sec response time of the super capacitor and 5 sec response time of the battery is obtained under worst-case load variations. Also, the DC bus is regulated to set a value with only 2.7 percent regulation, which is improved with respect to existing topologies, and the switching stress of the super capacitor is obtained to be only 1.6 percent with the proposed topology and Control. Another major factor is reduced battery interface inductor and power switch components, with a 93.75 percent reduction in inductor and an 83.33 percentage reduction in series switch voltage stress. Thus, the proposed work contributed to an efficient reduced-size hybrid power supply interface for PV-assisted electric vehicle drive. However, the limitations of the power conversion include complex operating modes with overlapping buck and boost conversion operations between the super capacitor and DC bus. With the merits of the cascaded converter, it could be extended for hybrid power conversion with other sources integrated at the front end.

References

[1] Eiad Saif, and İlyas Emınoğlu, "Hybrid Power Systems in Multi-Rotor UAVs: A Scientific Research and Industrial Production Perspective," *IEEE Access*, vol. 11, pp. 438-458, 2023. [CrossRef] [Google Scholar] [Publisher Link]

[2] Gyandeep Gurjar, D.K. Yadav and Seema Agrawal, "Illustration and Control of Nonisolated Multi-Input DC - DC Bidirectional Converter for Electric Vehicles using Fuzzy Logic Controller," *2020 IEEE International Conference for Innovation in Technology (INOCON)*, Bangalore, India, pp. 1-5, 2020. [CrossRef] [Google Scholar] [Publisher Link]

[3] Rouzbeh Reza Ahrabi et al., "A Novel Step-Up Multi-Input DC-DC Converter for Hybrid Electric Vehicles Application," *IEEE Transactions on Power Electronics*, vol. 32, no. 5, pp. 3549-3561, 2017. [CrossRef] [Google Scholar] [Publisher Link]

[4] Ujjal Manandhar et al., "Validation of Faster Joint Control Strategy for Battery- and Supercapacitor-Based Energy Storage System," *IEEE Transactions on Industrial Electronics*, vol. 65, no. 4, pp. 3286-3295, 2018. [CrossRef] [Google Scholar] [Publisher Link]

[5] Chun Gan et al., "Multiport Bidirectional SRM Drives for Solar-Assisted Hybrid Electric Bus Powertrain with Flexible Driving and Self-Charging Functions," *IEEE Transactions on Power Electronics*, vol. 33, no. 10, pp. 8231-8245, 2018. [CrossRef] [Google Scholar] [Publisher Link]

[6] Benfei Wang et al., "Bidirectional Three-Level Cascaded Converter with Deadbeat Control for HESS in Solar-Assisted Electric Vehicles," *IEEE Transactions on Transportation Electrification*, vol. 5, no. 4, pp. 1190-1201, 2019. [CrossRef] [Google Scholar] [Publisher Link]

[7] Chao Feng et al., "An Integrated BLIL Boost Converter-based Switched Reluctance Motor Drive for PEV Applications with PFC Charging Function," *2019 22nd International Conference on Electrical Machines and Systems (ICEMS)*, Harbin, China, pp. 1-5, 2019. [CrossRef] [Google Scholar] [Publisher Link]

[8] Ruoyun Shi, Sepehr Semsar, and Peter W. Lehn, "Single-Stage Hybrid Energy Storage Integration in Electric Vehicles using Vector Controlled Power Sharing," *IEEE Transactions on Industrial Electronics*, vol. 68, no. 11, pp. 10623-10633, 2021. [CrossRef] [Google Scholar] [Publisher Link]

[9] M.S. Okundamiya, "Size Optimization of a Hybrid Photovoltaic/Fuel Cell Grid-Connected Power System including Hydrogen Storage," *International Journal of Hydrogen Energy*, vol. 46, no. 59, pp. 30539-30546, 2021. [CrossRef] [Google Scholar] [Publisher Link]

[10] Gangavarapu Guru Kumar, and Kumaravel Sundaramoorthy, "Dual-Input Nonisolated DC-DC Converter with Vehicle-to-Grid Feature," *IEEE Journal of Emerging and Selected Topics in Power Electronics*, vol. 10, no. 3, pp. 3324-3336, 2022. [CrossRef] [Google Scholar] [Publisher Link]

[11] K. Suresh, and E. Parimalasundar, "Design and Implementation of Universal Converter Design and Implementation of a Universal Converter," *IEEE Canadian Journal of Electrical and Computer Engineering*, vol. 45, no. 3, pp. 272-278, Summer 2022. [CrossRef] [Google Scholar] [Publisher Link]

[12] Qingguo Sun et al., "Multiport PV-Assisted Electric-Drive-Reconstructed Bidirectional Charger with G2V and V2G/V2L Functions for SRM Drive-Based EV Application," *IEEE Journal of Emerging and Selected Topics in Power Electronics*, vol. 11, no. 3, pp. 3398-3408, 2023. [CrossRef] [Google Scholar] [Publisher Link]

[13] Vima Mali, and Brijesh Tripathi, "Thermal Stability of Supercapacitor for Hybrid Energy Storage System in Lightweight Electric Vehicles: Simulation and Experiments," *Journal of Modern Power Systems and Clean Energy*, vol. 10, no. 1, pp. 170-178, 2022. [CrossRef] [Google Scholar] [Publisher Link]

[14] Ramana Manohar Reddy, Moumita Das, and Nitin Chauhan, "Novel Battery-Supercapacitor Hybrid Energy Storage System for Wide Ambient Temperature Electric Vehicles Operation," *IEEE Transactions on Circuits and Systems II: Express Briefs*, vol. 70, no. 7, pp. 2580-2584, 2023. [CrossRef] [Google Scholar] [Publisher Link]

[15] Vaibhav Shah, and Saifullah Payami, "Integrated Converter with G2V, V2G, and DC/V2V Charging Capabilities for Switched Reluctance Motor Drive-Train based EV Application," *IEEE Transactions on Industry Applications*, vol. 59, no. 3, pp. 3837-3850, 2023. [CrossRef] [Google Scholar] [Publisher Link]

[16] Biswajit Saha, Bhim Singh, and Aryadip Sen, "Solar PV Integration to E-Rickshaw with Regenerative Braking and Sensorless Control," *IEEE Transactions on Industry Applications*, vol. 58, no. 6, pp. 7680-7691, 2022. [CrossRef] [Google Scholar] [Publisher Link]

[17] Xueqin Lü et al., "Energy Management of Hybrid Electric Vehicles: A Review of Energy Optimization of Fuel Cell Hybrid Power System based on Genetic Algorithm," *Energy Conversion and Management*, vol. 205, 2020. [CrossRef] [Google Scholar] [Publisher Link]

[18] Kaile Zhou et al., "A Coordinated Charging Scheduling Method for Electric Vehicles Considering Different Charging Demands," *Energy*, vol. 213, 2020. [CrossRef] [Google Scholar] [Publisher Link]

[19] Tianhong Wang et al., "Hierarchical Power Allocation Method based on Online Extremum Seeking Algorithm for Dual-PEMFC/Battery Hybrid Locomotive," *IEEE Transactions on Vehicular Technology*, vol. 70, no. 6, pp. 5679-5692, 2021. [CrossRef] [Google Scholar] [Publisher Link]

[20] Yu Yang, Hen-Geul Yeh, and Richard Nguyen, "A Robust Model Predictive Control-Based Scheduling Approach for Electric Vehicle Charging with Photovoltaic Systems," *IEEE Systems Journal*, vol. 17, no. 1, pp. 111-121, 2023. [CrossRef] [Google Scholar] [Publisher Link]

[21] Saurabh Mishra et al., "Driving-Cycle-Based Modeling and Control of Solar-Battery-Fed Reluctance Synchronous Motor Drive for Light Electric Vehicle with Energy Regeneration," *IEEE Transactions on Industry Applications*, vol. 58, no. 5, pp. 6666-6675, 2022. [CrossRef] [Google Scholar] [Publisher Link]

[22] Daeseong Park, and Mehdi Zadeh, "Modeling and Predictive Control of Shipboard Hybrid DC Power Systems," *IEEE Transactions on Transportation Electrification*, vol. 7, no. 2, pp. 892-904, 2021. [CrossRef] [Google Scholar] [Publisher Link]

[23] Zhumu Fu et al., "Energy Management Strategy for Fuel Cell/Battery/Ultracapacitor Hybrid Electric Vehicles using Deep Reinforcement Learning with Action Trimming," *IEEE Transactions on Vehicular Technology*, vol. 71, no. 7, pp. 7171-7185, 2022. [CrossRef] [Google Scholar] [Publisher Link]

[24] Daogui Tang, and Hongliang Wang, "Energy Management Strategies for Hybrid Power Systems Considering Dynamic Characteristics of Power Sources," *IEEE Access*, vol. 9, pp. 158796-158807, 2021. [CrossRef] [Google Scholar] [Publisher Link]

[25] C. Balasundar et al., "Interval Type2 Fuzzy Logic-Based Power Sharing Strategy for Hybrid Energy Storage System in Solar Powered Charging Station," *IEEE Transactions on Vehicular Technology*, vol. 70, no. 12, pp. 12450-12461, 2021. [CrossRef] [Google Scholar] [Publisher Link]

[26] Arian Zahedmanesh, Kashem M. Muttaqi, and Danny Sutanto, "A Cooperative Energy Management in a Virtual Energy Hub of an Electric Transportation System Powered by PV Generation and Energy Storage," *IEEE Transactions on Transportation Electrification*, vol. 7, no. 3, pp. 1123-1133, 2021. [CrossRef] [Google Scholar] [Publisher Link]